PAPER

Check for updates

A flexible Ti₃C₂Tₓ (MXene)/paper membrane for efficient oil/water separation†

Jayaprakash Saththasivam,[a] Kui Wang,[ab] Wubulikasimu Yiming, [c] Zhaoyang Liu [*a] and Khaled A. Mahmoud [*a]

The scalable fabrication of flexible membranes for efficient oil/water separation is in high demand but still significantly underdeveloped. Here, we present a flexible membrane using $Ti_3C_2T_x$ (MXene) as the functional layer on conventional print paper as the substrate. With a simple coating process using MXene ink, we developed a highly hydrophilic and oleophobic membrane with an underwater oil contact angle of 137°. Such a simple membrane shows outstanding flexibility and robustness, and demonstrates a facile approach for membrane scale-up using MXene ink on low-cost print paper. The membrane shows high separation efficiency for oil/water emulsions, of over 99%, and a high water permeation flux of over 450 L per m^2 per h per bar. We demonstrate the excellent anti-fouling property of this membrane by cleaning the membranes without chemicals. These low-cost, highly efficient, anti-fouling membranes can provide new opportunities for industrial oil/water separation applications.

1. Introduction

A large quantity of oily wastewater is produced on a daily basis from various oil industries, including production, refineries, shipping facilities, *etc.*[1] Technologies for treating oily wastewater are in great demand. Conventional technologies, including gravity settlement, hydrocyclone and air flotation, are not effective in separating emulsified oil/water mixtures, due to the small sizes of the oil droplets in these emulsions.[2] Membrane separation technologies, based on a "size sieving" mechanism, possess great potential in separating tiny oil droplets from water. However, most commercial membrane materials, like polyvinylidene fluoride (PVDF), polysulfone (PS), polypropylene (PP), or polytetrafluoroethylene (PTFE) are not hydrophilic, and thus suffer from serious membrane fouling issues, which inevitably cause a quick decline in permeation flux and separation efficiency.[3–9] This drawback leads to the limited adoption of these commercial membranes for treating large amounts of oily wastewater. Therefore, the development of new membranes with highly hydrophilic, underwater oleophobic and anti-fouling properties is crucial and in great demand for efficient oil/water separation in industry.[10–14]

With advances in nanomaterials and nanotechnology, new nanocomposites have been suggested to improve the effectiveness of oil/water separation membranes by adjusting the surface chemistry, roughness, and pore size.[4–8,15] Recently, a number of fabrication methods, such as surface grafting,[16–18] biomimetic adhesion,[19–21] and surface mineralization,[20,22,23] have been adopted to fabricate superwetting membranes with a hydrophilic (water-favoring) and underwater oleophobic (oil-repellent) layer on some substrates for oil/water separation. Several carbon-based nanocomposite membranes demonstrate promising efficiency in separation performance and anti-fouling property for various oil-in-water emulsion systems.[24–26] However, these newly-developed membranes are not suitable for scalable production due to their complexity and high-cost chemical preparation and membrane fabrication processes.

MXenes are a class of 2D nanomaterials from a large family of transition metal carbides, nitrides and carbonitrides.[27] Titanium carbide ($Ti_3C_2T_x$), where T_x denotes surface terminal groups (–OH, –O, and/or F), is the most widely studied member of the MXene family in water purification and environmental remediation applications due to its high surface area, hydrophilicity, surface functionality, abundance, facile scale-up synthesis, and environmentally benign characteristics.[28–30] MXenes have been also used extensively in water treatment applications, including water purification membranes,[31–33] heavy metal removal,[34,35] capacitive deionization,[36] and antimicrobial coatings.[37–39]

In this study, a new concept is explored to produce membranes with a simple and low-cost process by coating 2D $Ti_3C_2T_x$ (MXene) on commercial print paper, to achieve efficient separation of emulsified oil/water mixtures. These new membranes are produced by simple coating of $Ti_3C_2T_x$ MXene

ᵃQatar Environment and Energy Research Institute, Hamad Bin Khalifa University, Qatar Foundation, PO Box 34110, Doha, Qatar. E-mail: zliu@hbku.edu.qa; kmahmoud@hbku.edu.qa; Fax: +974 44541528

ᵇSchool of Traffic and Transportation Engineering, Central South University, Changsha 410075, China

ᶜChemical Engineering Program, Texas A&M University at Qatar, Education City, Doha 23874, Qatar

† Electronic supplementary information (ESI) available. See DOI: 10.1039/c9ra02129a

ink on commercial print paper as the substrate. These hydrophilic and densely packed 2D MXene nanoflakes will act as a functional layer for the efficient separation of emulsified oils, while the print paper substrate provides mechanical flexibility and strength. This very simple and yet novel membrane exhibits a good lifetime with less membrane fouling propensity and an easy membrane cleanup protocol. Moreover, the new concept demonstrates a simple and economic way for scalable fabrication of paper-based membranes for efficient separation of oil/water emulsions.

2. Methods

2.1. Materials

The commercial white print papers and sunflower oil that were used in this study were purchased locally. Hexane, silicone oil and petroleum ether were procured from VWR Chemicals (Radnor, PA, USA), Merck Millipore (Billerica, MA, USA) and Sigma-Aldrich (St. Louis, MO, USA), respectively. Ti_3AlC_2 (MAX) was purchased from Y-Carbon, Ltd., Ukraine. Other reagents are of analytical grade and were used as received. In all experiments, deionized (DI) water was used.

2.2. Synthesis of MXene

$Ti_3C_2T_x$ MXene was prepared from the MAX (Ti_3AlC_2) phase using 12 M lithium fluoride (LiF)/9 M hydrochloric acid (HCl) solution, following methods in the literature. The etching mixture was prepared by adding 0.8 g of LiF to 10 mL of 9 M HCl solution under continuous stirring for a period of five minutes. 0.5 g of Ti_3AlC_2 was added in small portions into the etching solution and kept under stirring for 24 h at room temperature to produce multi-layered (ML)-$Ti_3C_2T_x$. The synthesized material was centrifuged at 3500 rpm for five minutes and washed using deionized (DI) water in order to adjust the pH to within the range 4–5. The ML-$Ti_3C_2T_x$ solution was then probe sonicated in degassed water for one hour under inert conditions (using argon gas) at room temperature to produce delaminated (DL) $Ti_3C_2T_x$. The resulting solution was then centrifuged at 3500 rpm for 30 min and, finally, the supernatant was collected and freeze-dried and stored for preparation of the composite membrane.

2.3. Preparation of the composite membrane

MXene ink suspension at a concentration of 2 mg mL^{-1} was prepared by homogeneously dispersing the DL-MXene nanoflakes in deionized water using probe sonication for five minutes. The stock ink was then further diluted as per the required MXene mass loadings for membrane coating. The composite membrane was prepared by depositing the solution on commercial white print papers using a vacuum-assisted filtration setup.

2.4. Oil-in-water emulsion preparation

A stable 1% v/v oil-in-water emulsion was prepared as per the protocol described by Wang et al.[40] 10 mL of oil (e.g. sunflower oil, diesel, hexane, petroleum ether or silicon oil) was sonicated in 90 mL of deionized water for a period of five minutes using an

8510E-DTH ultrasonic bath (Danbury, CT, USA). The well-dispersed emulsion was then further diluted with 900 mL of deionized water to achieve a final concentration of 1% v/v. The prepared emulsion was stable over a long period, as no precipitation was observed even after several months.

2.5. Characterization

Surface and cross-sectional morphologies of the MXene-based composite membrane were studied using an FEI Quanta 400 (Hillsboro, OR, United States) environmental scanning electron microscope (ESEM). For imaging the cross-section, the composite membranes were cryo-fractured in liquid nitrogen. Transmission electronic microscopy (TEM) images of the MXene flakes were recorded using a bright field transmission electron microscope (TEM) (FEI Tecnai G2 TF20 UT). The samples were dispersed in water and mounted on a lacey carbon formvar coated Cu grid. The surface roughness of the composite membranes was characterized using an atomic force microscope (AFM, Bruker, USA). The water contact angle (WCA) and underwater oil contact angle (OCA) on the surface of the membranes were measured at room temperature using an advanced contact angle (CA) goniometer (Rame-hart model 500, Succasunna, NJ, USA). The WCA and hydrophilicity of the membranes were studied by analyzing the spreading process of water into the membranes where a high-speed camera with a speed of 100 frames/second was used to record the spreading process. As for the OCA measurement, the membranes were first immersed in distilled water. Oil droplets of 14 μL were then released from the bottom and allowed to rise to the surface of an MXene membrane immersed underwater. For all the contact angle measurements, an average of five measurements for two membrane samples was reported. The mechanical strength of the membranes was investigated at room temperature using a burst tester (TruBurst4, Halifax, England, UK). Circular membranes with testing areas of 7.3 cm^2 and a clamp pressure of 50 kPa were used in this study. The MXene-based membranes were deformed until the breakage point using compressed air operated at a constant pressure rate of 0.5 kPa s^{-1}. The deflection of the membrane center was recorded as a function of applied differential pressure.

2.6. Filtration performance testing

The oil/water separation efficiencies of the MXene-based composite membranes were evaluated using a glass filtration apparatus with an effective membrane area of 1.77 cm^2. The net trans-membrane pressure was maintained at 50 kPa using a diaphragm vacuum pump. Operating flux was calculated by measuring the volume of permeate passing through the membrane at a fixed filtration time. The oil content in the resulting permeate was measured using a total organic carbon analyzer (TOC-L, Shimadzu, Japan).

3. Results and discussions

The hierarchy of the deposited MXene nanoflakes on the print paper substrate is illustrated in Fig. 1(a). The delaminated
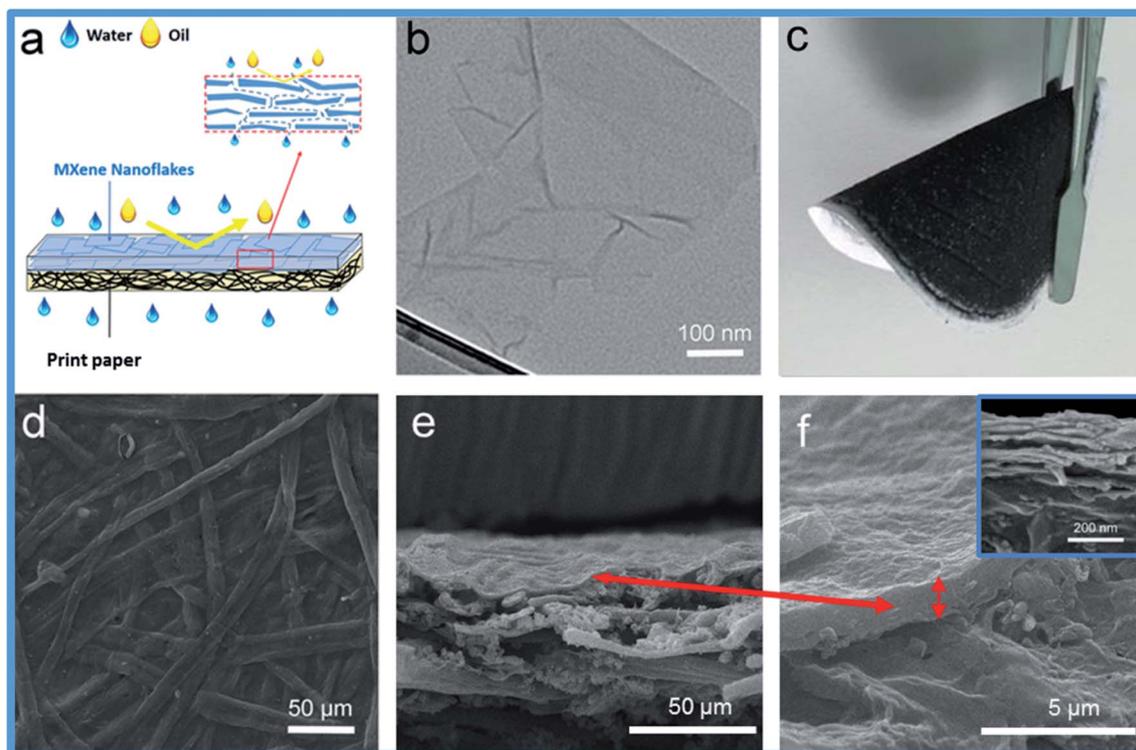
Fig. 1 (a) Schematic illustration of the deposited MXene nanoflakes on the polymeric fibers of commercial print paper. (b) TEM image of delaminated $Ti_3C_2T_x$ MXene. (c) Digital photograph demonstrating the flexibility of the MXene based composite membrane. (d) SEM image of substrate print paper. (e and f) Cross section SEM images of the MXene-based composite membranes at various magnification levels. The inset in (f) shows the layer-by-layer structure of MXene nanoflakes.

nanoflakes are stacked on the substrate, forming overlapping lamellar sheets that resulted in interlaced porous nanostructures. These stacks are expected to create multi-channel passages for water to flow through the membrane. The TEM image of $Ti_3C_2T_x$ MXene is exhibited in Fig. 1(b). In this figure, it can be observed that $Ti_3C_2T_x$ MXene can be exfoliated to a single sheet/few sheets, showing that the exfoliation process was effective.[41] The average sheet diameter can vary between 400 and 600 nm. Fig. 1(c) highlights the flexibility of the synthesized

composite membrane. The stacked structures of the MXene film enable the composite membrane to be folded without any cracking or disintegration. Surface morphological investigations of the composite membrane before and after MXene coating using SEM are shown in Fig. 1(d–f). It can be observed that the cellulose framework of print paper in Fig. 1(d) was evenly wrapped and covered by MXene nanoflakes, showing a more compact structure and continuous surface, as clearly shown in Fig. 1(e and f). Cross-section SEM images clearly show
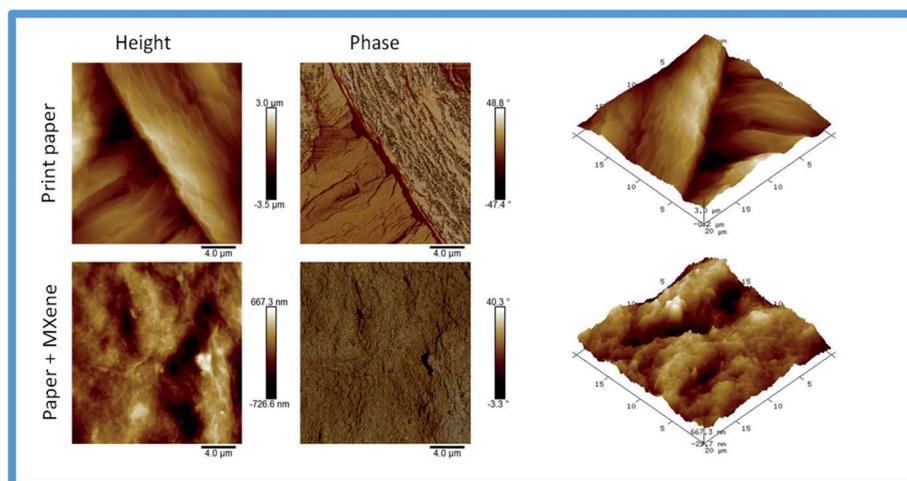

Fig. 2 Surface roughness comparison between the print paper substrate and the composite membrane.

the enlarged interplanar spacing of the stacked DL-MXene nanoflakes. The thickness of MXene film on the print paper substrate was 1.2 μm (inset, Fig. 1(f)).

XRD patterns of $Ti_3C_2T_x$ MXene are shown in the ESI.† The sharp and intense peak located at 2θ values of 7.2 can be assigned to the (002) plane of $Ti_3C_2T_x$ MXene. Other characteristic diffraction peaks at (004), (006), (008), and (0010) confirm the successful etching of aluminum layers from MAX and the delamination of multilayered MXene.

AFM analyses, shown Fig. 2, indicate that the print paper substrate had a root-mean-squared roughness (R_q) of 914 nm. With the deposition of MXene nanoflakes on print paper *via* vacuum filtration, the R_q decreased to 200 nm, suggesting the loss of microscale roughness for the print paper support. Lower surface roughness indicates a lower membrane fouling tendency after coating with MXene.

The hydrophilicity profile of the composite membrane over the time is described in Fig. 3(a). The water contact angle swiftly decreased to zero within two seconds of water droplet dispersion on the surface of the composite membrane, thus highlighting the excellent hydrophilicity of the composite membrane. The rapid water wetting phenomenon could be due to MXene's high affinity towards hydroxyl groups and the presence of interlaced porous nanoflakes that promote water passage.[31] The underwater oil contact angle, OCA, for the composite membrane, as shown in Fig. 3(b) was approximately 137° when tested using a sunflower oil droplet. This shows the great underwater oleophobicity properties of the MXene composite membrane.

Fig. 3(b) compares the mechanical strength of the MXene-based composite membrane *versus* the print paper substrate, which confirms that the composite membrane possesses better
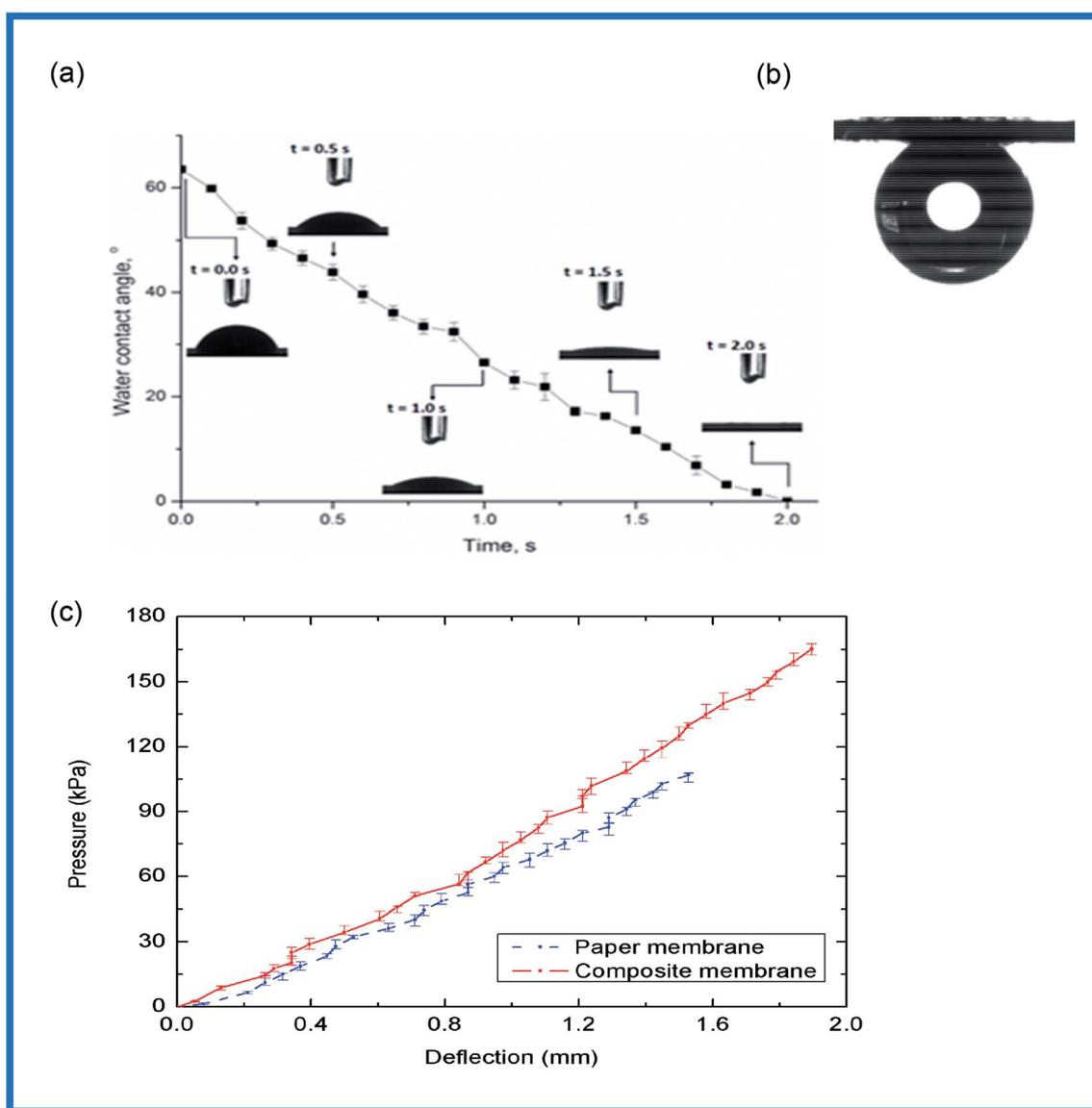

Fig. 3 (a) Rapid decrease in water contact angle observed in the composite membrane. (b) Underwater contact angle image indicating the underwater oleophobicity properties of the membrane. (c) Pressure–deflection curves of the MXene-based composite membrane.

mechanical strength and ductility due to its higher breakage pressure and deflection. The breakage pressure increased from 107.0 kPa to 165.1 kPa when the print paper was coated with delaminated MXene, which represents an increase of 54.3%. Similarly, the breakage deflection increased by 24.2% in the MXene-based composite membrane. The enhanced mechanical property of the MXene-based composite membrane is attributed to its more compact structure, resulting from the integration of MXene nanoflakes with cellulose papers that can also be observed from Fig. 1(f). The higher fracture response during mechanical loading could be due to effective interaction between the MXene nanoflakes and cellulose microfibers that benefited stress transfer and hence delayed the failure of the composite membrane.[42]

The performances of the MXene-based composite membrane in separating oil-in-water emulsion were evaluated by measuring the oil content in the permeate and operating flux. The composite membrane was optimized by varying the mass loadings of MXene deposited on the print paper. For this optimization test, the emulsified oil solution was prepared from sunflower oil due to its high viscosity.[43–45] The oil droplet size distribution of the emulsified sunflower oil ranged from 1 to 18 μm with a mean droplet size of 3.92 μm. Additional details on the oil droplet size distribution can be obtained in the ESI.† From Fig. 4, it can be observed that both permeation flux and oil content in the filtrates were inversely proportional to the mass loadings of MXene. The poor oil rejection rate of the porous commercial paper substrate without MXene loading was unsurprising, despite displaying a maximum flux of 2717.6 L per m^2 per h per bar. By increasing the mass loading of MXene from 0.1 mg to 0.8 mg, the flux of the composite membrane decreased fivefold from 1019.1 to 203.8 L per m^2 per h per bar. The oil rejection ratio in the filtrate improved by 98.5% as the

oil content in the filtrate dropped from 102.5 ppm to 1.6 ppm. By comparing the morphologies in Fig. 1(d) and (f), it can be confirmed that higher MXene loading leads to a more compact structure and a denser selective layer that in return reduce the flux and increase the permeate quality. In addition, the excellent hydrophilicity and underwater oleophobicity, as well as the interlaced porous structures of the composite membrane, contribute to the enhanced oil rejection rate. As the MXene loading was increased to 0.4 mg, the oil content in the permeate dropped below the requirement enacted by the US Environmental Protection Agency (USEPA) that permits the discharge of oil and grease in wastewater to a maximum of 42 ppm for any one day and a daily average lower than 26 ppm for 30 consecutive days. The corresponding flux and permeate quality at 0.4 mg of MXene loading were 543.5 L per m^2 per h per bar and 11.8 ppm. Further additions of MXene loadings (higher than 0.4 mg) lead to poorer water permeate flux. For subsequent studies, the MXene composite membranes were prepared using a mass loading of 0.4 mg MXene as an optimal composite.

The optimized MXene composite membranes that were prepared using a mass loading of 0.4 mg were also tested with four other different types of oil-in-water emulsion: namely (i) diesel, (ii) silicone oil, (iii) petroleum ether, and (iv) hexane. Fig. 5 shows the filtrate oil content and corresponding flux of the MXene composite membrane when challenged with these emulsions. The permeate flux ranges between 543.5 L per m^2 per h per bar and 682.3 L per m^2 per h per bar, where the highest flux was recorded for hexane, followed by petroleum ether, silicone oil, diesel and sunflower oil in a decreasing trend. As for the oil content in the filtrate, the levels for all the emulsions were less than 12 ppm, which is way below the allowable daily average limit of 26 ppm set by USEPA. It is worth mentioning that these high oil rejection ratios were achieved in a single pass
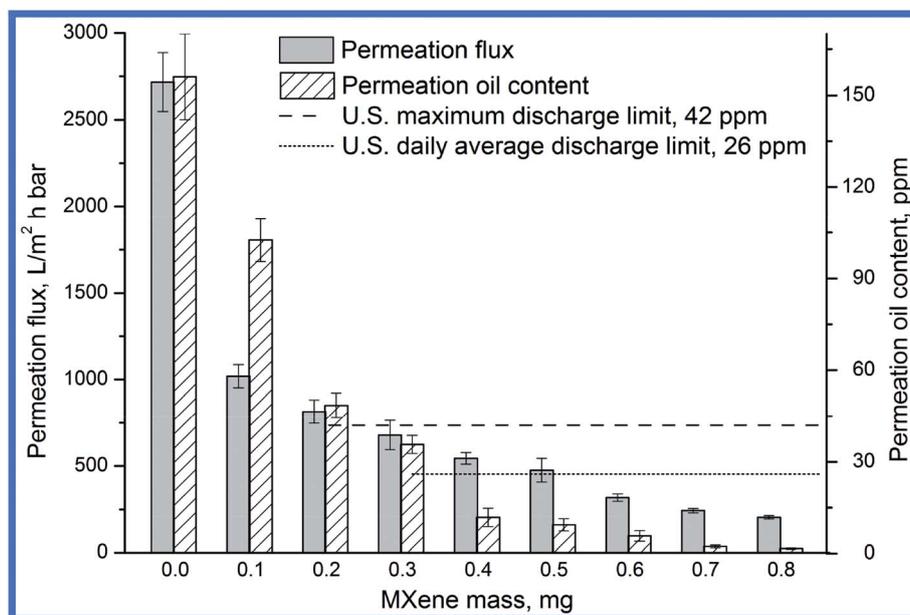

Fig. 4 Permeation fluxes and oil content in the filtrates of sunflower–oil-in-water emulsions filtrated by composite membranes prepared using different mass loadings of MXene.
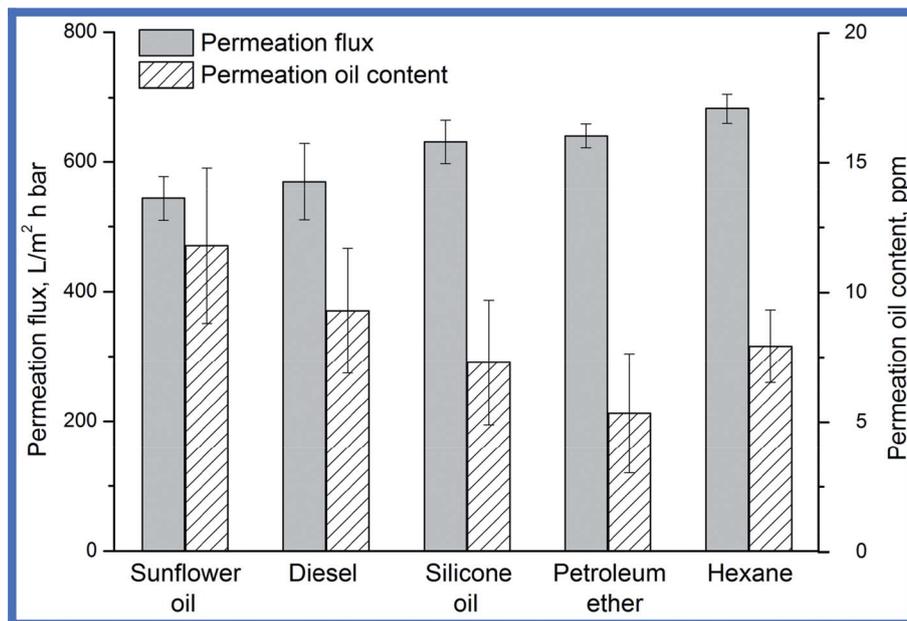
Fig. 5 Permeation fluxes and oil contents in the filtrates of five oil-in-water emulsions filtrated by the MXene based composite membrane.

with a low operating pressure of only 0.5 bar. Such separation performance is very attractive from the energy consumption perspective, since conventional oil/water membrane technologies operate at a higher transmembrane pressure.[46] The excellent permeation is most likely due to the synergy between hydrophilicity, underwater oleophobicity and the low oil-adhesion property of the membrane surface induced by the integration of MXene nanoflakes, as well as the interconnected porous structure.

The capability of an oil/water separation membrane to produce consistent water flux and permeate quality is of utmost importance for practical applications. In this study, we have investigated the reusability/recyclability of the MXene-based composite membrane in separating oil-in-water emulsion for several operating cycles. The membrane was flushed with hot water at the end of each filtration cycle to recover the flux. It can be observed in Fig. 6 that the operating flux of the composite membrane decreased only marginally after eight cycles of filtration. As for the oil separation efficiency, the oil content in the permeate was consistently lower than 11 ppm throughout all the filtration cycles, hence demonstrating an oil rejection efficiency of more than 99%. At the end of the eighth cycle, the
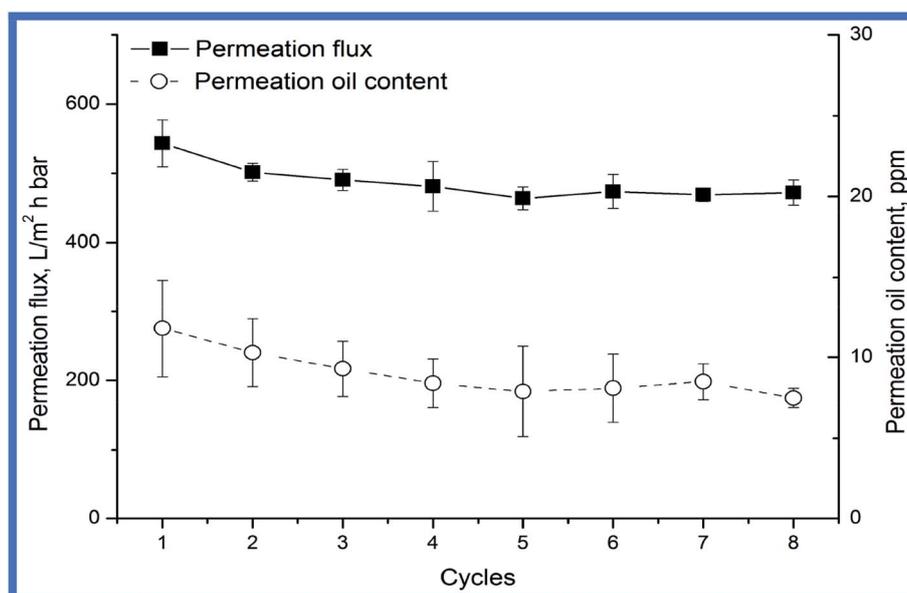

Fig. 6 Flux and permeate oil content of the MXene composite membrane over a period of eight operating cycles.

operating flux and permeate oil content of the MXene composite membrane were 472.1 L m^{-2} h^{-1} and 7.5 ppm, respectively. Surprisingly, even with commercial filter paper as substrate, the membrane remained intact with no sign of degradation even after 8 cycles of operation/washing steps. This is most likely due to high mechanical stability imposed by MXene film. Nevertheless, other substrates should be tested in the future to assure the long-term durability of the membranes. These results revealed that the MXene-based composite membrane featured excellent recyclability with anti-fouling property for emulsified oil-in-water separation, attributed to its high hydrophilicity and underwater oleophobicity properties. These favorable characteristics greatly mitigate fouling by facilitating the formation of a water layer that prevents direct interaction between the oil phase and the membrane surface during the separation process.[47,48]

4. Conclusion

In conclusion, we have demonstrated the fabrication of an efficient oil/water separating membrane through a simple and scalable coating process by coating 2D MXene ink onto everyday print paper. The print paper functions as a substrate to provide mechanical flexibility and strength, and the hydrophilic MXene layer functions as a selective layer to effectively separate emulsified oil from water. The new membrane demonstrated over 99% oil rejection efficiency while maintaining a high operating flux of 472.1 L m^{-2} h^{-1} after 8 consecutive cycles. Such MXene/paper-based membranes are flexible, robust and anti-fouling, and are excellent for oily wastewater treatment in various industries.

Conflicts of interest

There are no conflicts to declare.

Acknowledgements

References

1 Membrane and Desalination Technologies, ed. L. K. Wang, J. P. Chen, Y.-T. Hung and N. K. Shammas, Humana Press, Totowa, NJ, 2011, DOI: 10.1007/978-1-59745-278-6.
2 J. Saththasivam, K. Loganathan and S. Sarp, An Overview of Oil–water Separation Using Gas Flotation Systems, Chemosphere, 2016, 144, 671–680, DOI: 10.1016/j.chemosphere.2015.08.087.
3 D. Rana and T. Matsuura, Surface Modifications for Antifouling Membranes, Chem. Rev., 2010, 110(4), 2448–2471, DOI: 10.1021/cr800208y.
4 I. Sadeghi, A. Aroujalian, A. Raisi, B. Dabir and M. Fathizadeh, Surface Modification of Polyethersulfone Ultrafiltration Membranes by Corona Air Plasma for Separation of Oil/Water Emulsions, J. Membr. Sci., 2013, 430, 24–36, DOI: 10.1016/j.memsci.2012.11.051.
5 Y. Yang, H. Zhang, P. Wang, Q. Zheng and J. Li, The Influence of Nano-Sized TiO$_2$ Fillers on the Morphologies and Properties of PSF UF Membrane, J. Membr. Sci., 2007, 288(1–2), 231–238, DOI: 10.1016/j.memsci.2006.11.019.
6 W. Chen, Y. Su, L. Zheng, L. Wang and Z. Jiang, The Improved Oil/water Separation Performance of Cellulose Acetate-Graft-Polyacrylonitrile Membranes, J. Membr. Sci., 2009, 337(1–2), 98–105, DOI: 10.1016/j.memsci.2009.03.029.
7 J. Kong and K. Li, Oil Removal from Oil-in-Water Emulsions Using PVDF Membranes, Sep. Purif. Technol., 1999, 16(1), 83–93, DOI: 10.1016/S1383-5866(98)00114-2.
8 Y. S. Li, L. Yan, C. B. Xiang and L. J. Hong, Treatment of Oily Wastewater by Organic–inorganic Composite Tubular Ultrafiltration (UF) Membranes, Desalination, 2006, 196(1–3), 76–83, DOI: 10.1016/j.desal.2005.11.021.
9 X. S. Yi, S. L. Yu, W. X. Shi, N. Sun, L. M. Jin, S. Wang, B. Zhang, C. Ma and L. P. Sun, The Influence of Important Factors on Ultrafiltration of Oil/Water Emulsion Using PVDF Membrane Modified by Nano-Sized TiO$_2$/Al$_2$O$_3$, Desalination, 2011, 281, 179–184, DOI: 10.1016/j.desal.2011.07.056.
10 Z. Chu, Y. Feng and S. Seeger, Oil/Water Separation with Selective Superantiwetting/Superwetting Surface Materials, Angew. Chem., Int. Ed., 2015, 54(8), 2328–2338, DOI: 10.1002/anie.201405785.
11 B. Wang, W. Liang, Z. Guo and W. Liu, Biomimetic Super-Lyophobic and Super-Lyophilic Materials Applied for Oil/Water Separation: A New Strategy beyond Nature, Chem. Soc. Rev., 2015, 44(1), 336–361, DOI: 10.1039/c4cs00220b.
12 X. Yao, Y. Song and L. Jiang, Applications of Bio-Inspired Special Wettable Surfaces, Adv. Mater., 2011, 23(6), 719–734, DOI: 10.1002/adma.201002689.
13 T. Sun, L. Feng, X. Gao and L. Jiang, Bioinspired Surfaces with Special Wettability, Acc. Chem. Res., 2005, 38(8), 644–652, DOI: 10.1021/ar040224c.
14 J. Saththasivam, W. Yiming, K. Wang, J. Jin and Z. Liu, A Novel Architecture for Carbon Nanotube Membranes towards Fast and Efficient Oil/water Separation, Sci. Rep., 2018, 8(1), 7418, DOI: 10.1038/s41598-018-25788-9.
15 D. Qin, Z. Liu, D. Delai Sun, X. Song and H. Bai, A New Nanocomposite Forward Osmosis Membrane Custom-Designed for Treating Shale Gas Wastewater, Sci. Rep., 2015, 5(1), 14530, DOI: 10.1038/srep14530.
16 Y. Zhu, F. Zhang, D. Wang, X. F. Pei, W. Zhang and J. Jin, A Novel Zwitterionic Polyelectrolyte Grafted PVDF Membrane for Thoroughly Separating Oil from Water with Ultrahigh Efficiency, J. Mater. Chem. A, 2013, 1(18), 5758, DOI: 10.1039/c3ta01598j.
17 X. Zhao, Y. Su, W. Chen, J. Peng and Z. Jiang, Grafting Perfluoroalkyl Groups onto Polyacrylonitrile Membrane Surface for Improved Fouling Release Property, J. Membr.

Sci., 2012, **415–416**(415–416), 824–834, DOI: 10.1016/j.memsci.2012.05.075.

18 A. Rahimpour, S. S. Madaeni, S. Zereshki and Y. Mansourpanah, Preparation and Characterization of Modified Nano-Porous PVDF Membrane with High Antifouling Property Using UV Photo-Grafting, *Appl. Surf. Sci.*, 2009, **255**(16), 7455–7461, DOI: 10.1016/j.apsusc.2009.04.021.

19 H.-C. Yang, K.-J. Liao, H. Huang, Q.-Y. Wu, L.-S. Wan and Z.-K. Xu, Mussel-Inspired Modification of a Polymer Membrane for Ultra-High Water Permeability and Oil-in-Water Emulsion Separation, *J. Mater. Chem. A*, 2014, **2**(26), 10225–10230, DOI: 10.1039/c4ta00143e.

20 H.-C. Yang, J.-K. Pi, K.-J. Liao, H. Huang, Q.-Y. Wu, X.-J. Huang and Z.-K. Xu, Silica-Decorated Polypropylene Microfiltration Membranes with a Mussel-Inspired Intermediate Layer for Oil-in-Water Emulsion Separation, *ACS Appl. Mater. Interfaces*, 2014, **6**(15), 12566–12572, DOI: 10.1021/am502490j.

21 S. Kasemset, A. Lee, D. J. Miller, B. D. Freeman and M. M. Sharma, Effect of Polydopamine Deposition Conditions on Fouling Resistance, Physical Properties, and Permeation Properties of Reverse Osmosis Membranes in Oil/Water Separation, *J. Membr. Sci.*, 2013, **425–426**, 208–216, DOI: 10.1016/j.memsci.2012.08.049.

22 P.-C. Chen and Z.-K. Xu, Mineral-Coated Polymer Membranes with Superhydrophilicity and Underwater Superoleophobicity for Effective Oil/Water Separation, *Sci. Rep.*, 2013, **3**(1), 2776, DOI: 10.1038/srep02776.

23 X. Zhao, Y. Su, J. Cao, Y. Li, R. Zhang, Y. Liu and Z. Jiang, Fabrication of Antifouling Polymer–Inorganic Hybrid Membranes through the Synergy of Biomimetic Mineralization and Nonsolvent Induced Phase Separation, *J. Mater. Chem. A*, 2015, **3**(14), 7287–7295, DOI: 10.1039/c5ta00654f.

24 X. Zhao, Y. Su, Y. Liu, Y. Li and Z. Jiang, Free-Standing Graphene Oxide-Palygorskite Nanohybrid Membrane for Oil/Water Separation, *ACS Appl. Mater. Interfaces*, 2016, **8**(12), 8247–8256, DOI: 10.1021/acsami.5b12876.

25 F. Perreault, M. E. Tousley and M. Elimelech, Thin-Film Composite Polyamide Membranes Functionalized with Biocidal Graphene Oxide Nanosheets, *Environ. Sci. Technol. Lett.*, 2014, **1**(1), 71–76, DOI: 10.1021/ez4001356.

26 J. Zhang, Q. Xue, X. Pan, Y. Jin, W. Lu, D. Ding and Q. Guo, Graphene Oxide/Polyacrylonitrile Fiber Hierarchical-Structured Membrane for Ultra-Fast Microfiltration of Oil-Water Emulsion, *Chem. Eng. J.*, 2017, **307**, 643–649, DOI: 10.1016/j.cej.2016.08.124.

27 J.-C. Lei, X. Zhang and Z. Zhou, Recent Advances in MXene: Preparation, Properties, and Applications, *Front. Phys.*, 2015, **10**(3), 276–286, DOI: 10.1007/s11467-015-0493-x.

28 M. Naguib, M. Kurtoglu, V. Presser, J. Lu, J. Niu, M. Heon, L. Hultman, Y. Gogotsi and M. W. Barsoum, Two-Dimensional Nanocrystals Produced by Exfoliation of Ti_3AlC_2, *Adv. Mater.*, 2011, **23**(37), 4248–4253, DOI: 10.1002/adma.201102306.

29 X. Zheng, R. Wu and Y. Chen, Effects of ZnO Nanoparticles on Wastewater Biological Nitrogen and Phosphorus Removal, *Environ. Sci. Technol.*, 2011, **45**(7), 2826–2832, DOI: 10.1021/es2000744.

30 Q. Zhang, J. Teng, G. Zou, Q. Peng, Q. Du, T. Jiao and J. Xiang, Efficient Phosphate Sequestration for Water Purification by Unique Sandwich-like MXene/Magnetic Iron Oxide Nanocomposites, *Nanoscale*, 2016, **8**(13), 7085–7093, DOI: 10.1039/c5nr09303a.

31 R. Han, X. Ma, Y. Xie, D. Teng and S. Zhang, Preparation of a New 2D MXene/PES Composite Membrane with Excellent Hydrophilicity and High Flux, *RSC Adv.*, 2017, **7**(89), 56204–56210, DOI: 10.1039/c7ra10318b.

32 R. P. Pandey, K. Rasool, P. Abdul Rasheed and K. A. Mahmoud, Reductive Sequestration of Toxic Bromate from Drinking Water Using Lamellar Two-Dimensional $Ti_3C_2T_X$ (MXene), *ACS Sustainable Chem. Eng.*, 2018, **6**(6), 7910–7917, DOI: 10.1021/acssuschemeng.8b01147.

33 C. E. Ren, K. B. Hatzell, M. Alhabeb, Z. Ling, K. A. Mahmoud and Y. Gogotsi, Charge- and Size-Selective Ion Sieving Through $Ti_3C_2T_X$ MXene Membranes, *J. Phys. Chem. Lett.*, 2015, **6**(20), 4026–4031, DOI: 10.1021/acs.jpclett.5b01895.

34 A. Shahzad, K. Rasool, W. Miran, M. Nawaz, J. Jang, K. A. Mahmoud and D. S. Lee, Two-Dimensional $Ti_3C_2T_X$ MXene Nanosheets for Efficient Copper Removal from Water, *ACS Sustainable Chem. Eng.*, 2017, **5**(12), 11481–11488, DOI: 10.1021/acssuschemeng.7b02695.

35 Y. Ying, Y. Liu, X. Wang, Y. Mao, W. Cao, P. Hu and X. Peng, Two-Dimensional Titanium Carbide for Efficiently Reductive Removal of Highly Toxic Chromium(VI) from Water, *ACS Appl. Mater. Interfaces*, 2015, **7**(3), 1795–1803, DOI: 10.1021/am5074722.

36 P. Srimuk, F. Kaasik, B. Krüner, A. Tolosa, S. Fleischmann, N. Jäckel, M. C. Tekeli, M. Aslan, M. E. Suss and V. Presser, MXene as a Novel Intercalation-Type Pseudocapacitive Cathode and Anode for Capacitive Deionization, *J. Mater. Chem. A*, 2016, **4**(47), 18265–18271, DOI: 10.1039/c6ta07833h.

37 K. Rasool, M. Helal, A. Ali, C. E. Ren, Y. Gogotsi and K. A. Mahmoud, Antibacterial Activity of $Ti_3C_2T_X$ MXene, *ACS Nano*, 2016, **10**(3), 3674–3684, DOI: 10.1021/acsnano.6b00181.

38 K. Rasool, K. A. Mahmoud, D. J. Johnson, M. Helal, G. R. Berdiyorov and Y. Gogotsi, Efficient Antibacterial Membrane Based on Two-Dimensional $Ti_3C_2T_x$ (MXene) Nanosheets, *Sci. Rep.*, 2017, **7**(1), 1598, DOI: 10.1038/s41598-017-01714-3.

39 R. P. Pandey, K. Rasool, V. E. Madhavan, B. Aïssa, Y. Gogotsi and K. A. Mahmoud, Ultrahigh-Flux and Fouling-Resistant Membranes Based on Layered Silver/MXene ($Ti_3C_2T_X$) Nanosheets, *J. Mater. Chem. A*, 2018, **6**(8), 3522–3533, DOI: 10.1039/c7ta10888e.

40 K. Wang, W. Yiming, J. Saththasivam and Z. Liu, A Flexible, Robust and Antifouling Asymmetric Membrane Based on Ultra-Long Ceramic/Polymeric Fibers for High-Efficiency Separation of Oil/Water Emulsions, *Nanoscale*, 2017, **9**(26), 9018–9025, DOI: 10.1039/c7nr02364b.

41 Y. Cao, Q. Deng, Z. Liu, D. Shen, T. Wang, Q. Huang, S. Du, N. Jiang, C. T. Lin and J. Yu, Enhanced Thermal Properties of Poly(vinylidene fluoride) Composites with Ultrathin Nanosheets of MXene, *RSC Adv.*, 2017, **7**(33), 20494–20501, DOI: 10.1039/c7ra00184c.

42 K. Wang, A. A. Abdalla, M. A. Khaleel, N. Hilal and M. K. Khraisheh, Mechanical Properties of Water Desalination and Wastewater Treatment Membranes, *Desalination*, 2017, **401**, 190–205, DOI: 10.1016/j.desal.2016.06.032.

43 S. J. Gao, Z. Shi, W. B. Zhang, F. Zhang and J. Jin, Photoinduced Superwetting Single-Walled Carbon Nanotube/TiO$_2$ Ultrathin Network Films for Ultrafast Separation of Oil-in-Water Emulsions, *ACS Nano*, 2014, **8**(6), 6344–6352, DOI: 10.1021/nn501851a.

44 A. Demirbaş, Biodiesel Fuels from Vegetable Oils via Catalytic and Non-Catalytic Supercritical Alcohol Transesterifications and Other Methods: A Survey, *Energy Convers. Manage.*, 2003, **44**, 2093–2109, DOI: 10.1016/S0196-8904(02)00234-0.

45 A. Demirbas, Biodiesel from Sunflower Oil in Supercritical Methanol with Calcium Oxide, *Energy Convers. Manage.*, 2007, **48**(3), 937–941, DOI: 10.1016/j.enconman.2006.08.004.

46 W. Zhang, Y. Zhu, X. Liu, D. Wang, J. Li, L. Jiang and J. Jin, Salt-Induced Fabrication of Superhydrophilic and Underwater Superoleophobic PAA-G-PVDF Membranes for Effective Separation of Oil-in-Water Emulsions, *Angew. Chem., Int. Ed.*, 2014, **53**(3), 856–860, DOI: 10.1002/anie.201308183.

47 Y. Huang, H. Li, L. Wang, Y. Qiao, C. Tang, C. Jung, Y. Yoon, S. Li and M. Yu, Ultrafiltration Membranes with Structure-Optimized Graphene-Oxide Coatings for Antifouling Oil/Water Separation, *Adv. Mater. Interfaces*, 2015, **2**(2), 1400433, DOI: 10.1002/admi.201400433.

48 Z. Xue, Y. Cao, N. Liu, L. Feng and L. Jiang, Special Wettable Materials for Oil/Water Separation, *J. Mater. Chem. A*, 2014, **2**(8), 2445–2460, DOI: 10.1039/c3ta13397d.